Applied Surface Science 257 (2011) 5913–5918

Contents lists available at ScienceDirect

Applied Surface Science

journal homepage: www.elsevier.com/locate/apsusc

Enhanced corrosion resistance and cellular behavior of ultrafine-grained biomedical NiTi alloy with a novel SrO–SiO_2–TiO_2 sol–gel coating

C.Y. Zheng[a,b], F.L. Nie[a,b], Y.F. Zheng[a,b,*], Y. Cheng[b], S.C. Wei[c,**], Liqun Ruan[d], R.Z. Valiev[e]

[a] State Key Laboratory for Turbulence and Complex System and Department of Advanced Materials and Nanotechnology, College of Engineering, Peking University, Beijing 100871, China
[b] Center for Biomedical Materials and Tissue Engineering, Academy for Advanced Interdisciplinary Studies, Peking University, Beijing 100083, China
[c] Department of Oral and Maxillofacial Surgery, School of Stomatology, Peking University, Beijing 100081, China
[d] Department of Mechanical Systems Engineering, Graduate School of Science and Technology, Kumamoto University, Kurokami 2-39-1, Kumamoto-shi 860-8555, Japan
[e] Institute of Physics of Advanced Materials, Ufa State Aviation Technical University, Ufa, Russia

ARTICLE INFO

Article history:
Received 19 January 2011
Received in revised form 1 February 2011
Accepted 1 February 2011
Available online 20 February 2011

Keywords:
Ultrafine-grained NiTi
Sol–gel coating
Cytocompatibility
Corrosion resistance

ABSTRACT

NiTi alloy has a unique combination of mechanical properties, shape memory effects and superelastic behavior that makes it attractive for several biomedical applications. In recent years, concerns about its biocompatibility have been aroused due to the toxic or side effect of released nickel ions, which restricts its application as an implant material. Bulk ultrafine-grained Ni50.8Ti49.2 alloy (UFG NiTi) was successfully fabricated by equal-channel angular pressing (ECAP) technique in the present study. A homogeneous and smooth SrO–SiO_2–TiO_2 sol–gel coating without cracks was fabricated on its surface by dip-coating method with the aim of increasing its corrosion resistance and cytocompatibility. Electrochemical tests in simulated body fluid (SBF) showed that the pitting corrosion potential of UFG NiTi was increased from 393 mV(SCE) to 1800 mV(SCE) after coated with SrO–SiO_2–TiO_2 film and the corrosion current density decreased from 3.41 $\mu A/cm^2$ to 0.629 $\mu A/cm^2$. Meanwhile, the sol–gel coating significantly decreased the release of nickel ions of UFG NiTi when soaked in SBF. UFG NiTi with SrO–SiO_2–TiO_2 sol–gel coating exhibited enhanced osteoblast-like cells attachment, spreading and proliferation compared with UFG NiTi without coating and CG NiTi.

1. Introduction

In recent years, NiTi alloy is known as a material with a unique combination of mechanical properties, shape memory effects, superelastic behavior, corrosion resistance and biocompatibility that makes it attractive for several biomedical applications such as dental archwires, surgical retractors, bone staples and endoscopic instruments [1]. With development of severe plastic deformation (SPD) techniques, including high-pressure torsion [2,3], equal-channel angular pressing [2,4,5] and multi-step SPD deformation (SPD plus cold rolling or drawing) [2,6], pure metals or alloys with ultrafine grains achieved by SPD process with subsequent annealing show superior mechanical properties, such as high strength and improved ductility, as well as lower temperature and higher strain rate superplasticity [7]. Recently, ultrafine-grained (UFG) NiTi alloys processed by ECAP technique demonstrated higher strength (yield stress up to 1300 MPa) as well as enhanced functional properties (maximum recovery stress to 1100 MPa and maximum fully recoverable strain to 9.2%) compared to the coarse-grained counterparts [2,4]. Moreover, very recent work on ultrafine-grained NiTi showed higher corrosion resistance and equivalent cytocompatibility either within L-929 or MG 63 culture compared with microcrystalline NiTi alloy by the present authors [8]. Thus, UFG NiTi with high strength and functional properties as well as better biocompatibility, seems to be favorable for future applications as a biomaterial.

Even though the protective oxide film exists on the surface of NiTi alloy implants, Ni ions can still be released to the surround tissue when implanted, which might induce allergic reaction, and if above a certain concentration would lead to severe local tissue irritation, necrosis and toxic reactions. At the same time, NiTi alloy with relatively low pitting potential values exhibits poor resistance to localized corrosion in chloride-containing environments [9]. In addition, the healing of the passive film on NiTi alloy has been reported to be a slow and difficult process. Therefore, surface modification are employed to increase the corrosion resistance of NiTi alloy and make it more biocompatible, thereby improving

* Corresponding author at: Department of Advanced Materials and Nanotechnology, College of Engineering, Peking University, Beijing 100871, China.
Tel.: +86 10 6276 7411; fax: +86 10 6276 7411.
** Co-corresponding author.
E-mail address: yfzheng@pku.edu.cn (Y.F. Zheng).

0169-4332/$ – see front matter © 2011 Elsevier B.V. All rights reserved.
doi:10.1016/j.apsusc.2011.02.006

its long-term stability. Concerning the high Ni content, the high sensitivity of NiTi alloy to heat treatment, and possible complex shapes of implants, special requirements on the surface treatment techniques for NiTi alloy are imposed. Especially, as to UFG NiTi, heat treatment at high temperature or other treatment which would cause sharp increase of the substrate temperature should be avoided to protect the unltrafine-grained structure and keep its mechanical properties unchanged. Sol–gel technology is a low temperature method of producing metallic oxide glass, bioceramics and bioactive titania-like surfaces from chemical routes. It has been previously demonstrated that sol–gel films such as TiO_2, TiO_2–SiO_2 and SiO_2–Al_2O_3 composite sol–gel coatings of NiTi alloy and 316L stainless steel as protective coatings against corrosion were very effective [10–13]. Sol–gel coatings on biometal have also exhibited good bioactivity due to abundant hydroxyl (OH) groups on the surface that promote nucleation of calcium apatite or formation of mineralized matrix by osteoblasts [14,15].

In the present work, a novel SrO–SiO_2–TiO_2 sol–gel coating was developed due to the beneficial effect of strontium on bone formation and healing osteoporotic tissues [16]. Ultrafine-grained biomedical NiTi alloy was coated with the above sol–gel coating in the first instance with the aim of increasing its corrosion resistance and cytocompitability. The effect of the coating on the in vitro biocompatibility of UFG NiTi such as corrosion resistance, ion release and cellular behavior were studied.

2. Materials and methods

2.1. Surface modification

Ultrafine-grained NiTi (50.8 at.% Ni, dubbed UFG NiTi) was prepared by ECAP technique from commercial coarse-grained Ni50.8Ti49.2 (dubbed CG-NiTi) bars with a diameter of 20 mm (both provided by Ufa State Aviation Technical University) with subsequent anneal in vacuum at a temperature of 300 °C for 30 min. It has equiaxed grains with a mean grain size of 200–300 nm. Rectangular strips with typical dimensions of 10 mm × 10 mm × 1.5 mm were cut by spark-erosion wire cutting, ground with SiC paper up to 2000 grit, and cleaned ultrasonically in acetone for 10 min, in ethanol for 10 min and in distilled water for 10 min in turn, then dried at 40 °C in a dryer.

SrO–SiO_2–TiO_2 sol was achieved by mixing TiO_2 sol and SrO–SiO_2 sol, then dip-coated onto UFG NiTi substrates. TiO_2 sol was prepared as follows: titanium tetraisopropoxide (TTIP) was dissolved into ethanol (EtOH) and mixed with the solution containing acetylacetone (Acac), deionized water, hydrochloric acid (HCl, 37%). The sol was aged for 6 h at room temperature of ~22 °C. The SrO–SiO_2 sol was prepared as follows: tetraethoxysilane (TEOS) was dissolved into ethanol and mixed with the solution containing strontium nitrate, distilled water and hydrochloric acid (HCl, 37%). The sol was aged for 6 h at room temperature. Then, the TiO_2 sol was mixed with SrO–SiO_2 sol, and aged for 12 h at 4 °C to obtain SrO–SiO_2–TiO_2 sol for dip-coating process. All the above sols were prepared under stirring conditions, and the volumetric ratio was controlled to make sure that the molar ratio of SrO:SiO_2:TiO_2 was 3:25:72.

UFG NiTi samples were dipped into the SrO–SiO_2–TiO_2 sol and withdrawn at a speed of 5 mm/min at room temperature. The resulting samples were dried at room temperature, 50 °C, 100 °C, 150 °C for 30 min in turn. This dip-coating-drying step was repeated for five times. Then they were hydrothermally treated at 200 °C for 8 h according to reference [17] to avoid high temperature heat treatment. The thickness of the resulting coating is about 200 nm, similar to the literatures [18,19].

2.2. Corrosion behavior

The electrochemical corrosion measurements were performed using an electrochemical workstation (CHI600C, China) at room temperature. The electrolyte was simulated body fluid (SBF) proposed by Kokubo without organic species [20]. The ion concentrations are as follows: Na^+ 142.0, K^+ 5.0, Mg^{2+} 1.5, Ca^{2+} 2.5, HCO_3^- 4.2, Cl^- 147.8, HPO_4^{2-} 1.0, SO_4^{2-} 0.5 mM, which is nearly equal to those of human blood plasma except HCO_3^- being 27.0 mM. The sample was set as a working electrode, a platinum electrode acting as an auxiliary electrode and the reference electrode a saturated calomel electrode (SCE). The OCP (open circuit potential) measurement was maintained up to 7200 s. Potentiodynamic polarization curves were then measured from −800 mV (vs. SCE) to 2000 mV (vs. SCE) with a scan rate of 1 mV/s.

Concerns about the potential risk associated with corrosion of NiTi alloy has been reported due to the biological side effects of Ni. Nickel ions release was measured by immersion test. UFG NiTi alloy plates with and without sol–gel coating were immersed in SBF at 37 ± 0.5 °C for 28 days. The inductively coupled plasma atomic emission spectrometry (Leeman, Profile ICP-AES) was utilized to determine the amount of Ni ions.

2.3. Cell experiment

Cell adhesion and proliferation tests were performed with osteoblast-like cell line MG63 (CRL1427, ATCC, USA). Before performing these assays, the cells were cultured in MEM medium (Invitrogen) supplemented with 10% of fetal calf serum and 1% penicillin/streptomycin at 37 °C in a humidified atmosphere of 5% CO_2 in air. MG63 cells were seeded onto the CG-NiTi, UFG NiTi and sol–gel coated UFG NiTi samples in 24-well culture plates at a density of 5×10^4 cells $well^{-1}$ for direct cell adhesion observation. After 4 h and 3 days incubation, the culture media were removed and specimens were fixed with 2.5% glutaraldehyde solution for 1 h at room temperature and rinsed 3 times with phosphate buffer solution (PBS, pH 7.4), followed by dehydration in a gradient ethanol/distilled water mixture (50%, 60%, 70%, 80%, 90%, 100%) for 10 min and dried in air. Samples were sputter coated with gold for cell morphology observation using environmental scanning electron microscope (ESEM, AMRAY-1910FE).

2.4. Surface characterization

Before and after electrochemical tests, the surface morphology and composition of UFG NiTi with and without sol–gel coating were assessed by ESEM equipped with an energy dispersive spectrometer (EDS) and analyzed by X-ray diffractometer (XRD) using a Rigaku DMAX 2400 diffractometer with Cu Kα irradiation. The powders of dried SrO–SiO_2–TiO_2 gel with subsequent hydrothermal treatment at 200 °C for 8 h were characterized by XRD. Fourier transform infrared spectroscopy (FTIR, Nicolett Magna-IR 750) of the powders was obtained by mixing with KBr powders with pressed-disc process at transmission mode.

3. Results and discussion

3.1. Surface morphology and composition of sol–gel coated UFG NiTi alloy

The surface morphology of UFG NiTi with sol–gel coating was shown in Fig. 1. Compared to the ground UFG NiTi sample with characteristics of grinding scratches (Fig. 1(a)), UFG NiTi with SrO–SiO_2–TiO_2 coating were morphologically smooth and free of

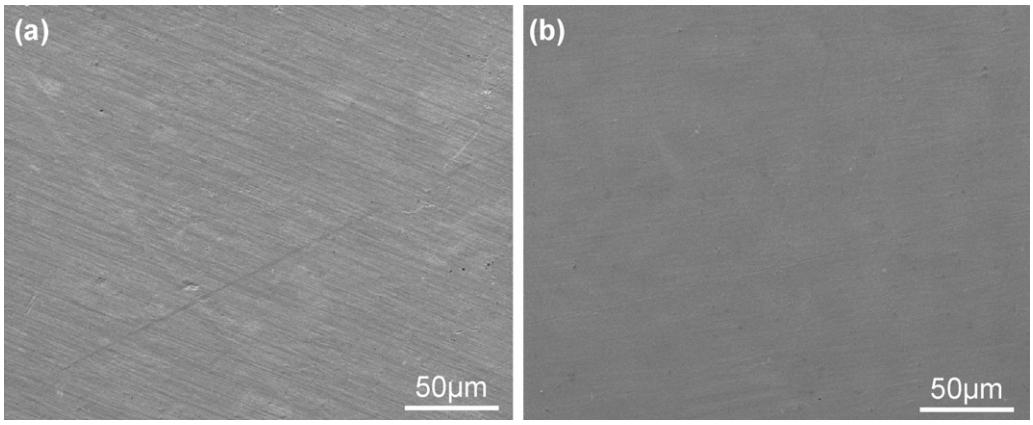

Fig. 1. SEM surface morphologies of UFG NiTi before (a) and after (b) SrO–SiO_2–TiO_2 sol–gel coating.

cracks (Fig. 1(b)). The coating is too thin to be detected by XRD analysis in Fig. 2. However, the powders of dried SrO–SiO_2–TiO_2 gel with subsequent hydrothermal treatment at 200 °C for 8 h consists of anatase, which, on the other hand, show the sol–gel coating on UFG NiTi was mainly anatase. SiO_2 was probably amorphous since no signals of crystallized silica were observed, which was similar to the results of others. Jeon et al. [21] found that the matrix of Ag–SiO_2 sol–gel coating heat-treated in the temperature range from 200 °C to 600 °C was amorphous SiO_2. Jokinen et al. [18] reported that the structure of sol–gel derived TiO_2–SiO_2 film calcined at 500 °C was amorphous with a little anatase precipitated.

Fig. 3 shows the FTIR spectra of powders of dried SrO–SiO_2–TiO_2 gel with subsequent hydrothermal treatment. The bands observed at 460 cm^{-1} and 1070 cm^{-1} corresponded to the Si–O bands [11]. Ti–O bands were observed at 1395 cm^{-1} and 1716 cm^{-1} [22]. The band at 940 cm^{-1} and 1627 cm^{-1} were assigned to Si–O–Ti and O–H bands respectively [11]. The band at 800 cm^{-1} is linked to the ring structure [11,14]. In this study, it attributed to Si–O–Ti, Si–O–Si and Sr–O–Si. During sol–gel preparation, the main reactions occurring in the system due to hydrolysis and condensation are the following:

$$Ti(OC_4H_9)_4 + 4H_2O \rightarrow Ti(OH)_4 + 4C_4H_9OH \quad (1)$$

$$Si(OC_2H_5)_4 + 4H_2O \rightarrow Si(OH)_4 + 4C_2H_5OH \quad (2)$$

$$Si(OH)_4 + Si(OH)_4 \rightarrow (OH)_3Si{-}O{-}Si(OH)_3 + H_2O \quad (3)$$

$$(OH)_3Si{-}O{-}Si(OH)_3 + 6Si(OH)_4 \rightarrow [(OH)_3SiO]_3Si{-}O{-}Si[OSi(OH)_3]_3 + 6H_2O \quad (4)$$

$$Si(OC_2H_5)_4 + H_2O \rightarrow Si(OH)(OC_2H_5)_3 + C_2H_5OH \quad (5)$$

$$2Si(OH)(OC_2H_5)_3 + Sr(NO_3)_2 \rightarrow Sr[OSi(OC_2H_5)_3]_4 + 2HNO_3 \quad (6)$$

$$4Si(OH)(OC_2H_5)_3 + Ti(OH)_4 \rightarrow Ti[OSi(OC_2H_5)_3]_4 + 4H_2O \quad (7)$$

Ti–O and Si–O bands formed as Eqs. (1) and (2) shows respectively. Reactions as in (3) and (4) led to the formation of Si–O–Si. Sr–O–Si band was attributed to reactions as in (5) and (6), while the generation of Ti–O–Si was on account of the hydrolysis and condensation reactions as in (5) and (7). The dip-coated sol–gel coating was then densified and crystallized during subsequent drying and hydrothermal treatment achieving a homogeneous SrO–SiO_2–TiO_2 coating.

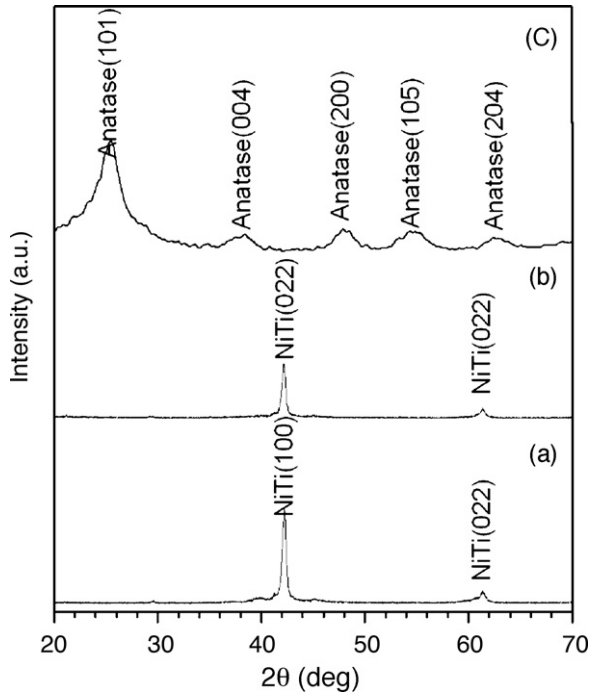

Fig. 2. XRD profiles of (a) UFG NiTi, (b) UFG NiTi with SrO–SiO_2–TiO_2 sol–gel coating and (c) powders of dried SrO–SiO_2–TiO_2 gel.

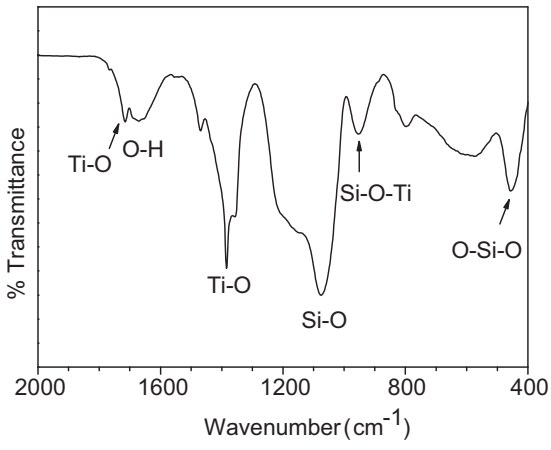

Fig. 3. FTIR spectrum of powders of dried SrO–SiO_2–TiO_2 gel with subsequent hydrothermal treatment.

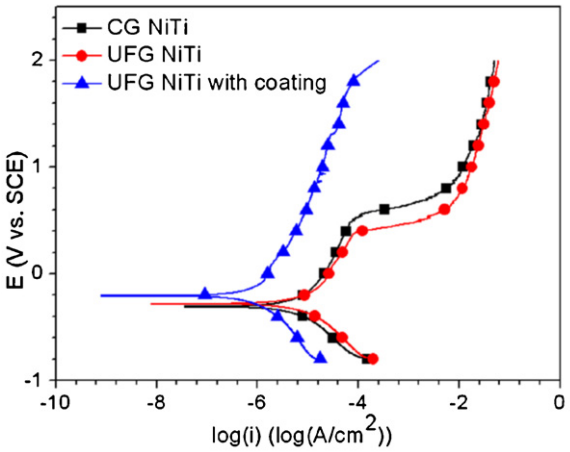

Fig. 4. Potentiodynamic polarization curves of CG NiTi and UFG NiTi with and without $SrO–SiO_2–TiO_2$ sol–gel coating.

3.2. Corrosion behavior

The corrosion behavior of NiTi alloy in physiological environments has been reported and the results are rather controversial [23]. Either no pitting corrosion or an earlier breakdown of its passive film as well as an intermediate pitting potential (~800 mV(SCE)) inferior to Ti6Al4 V (>1000 mV(SCE)) but superior to AISI 316L (~400 mV(SCE)) during potentiodynamic tests has been recorded [9,23–25]. The potentiodynamic polarization behaviors of UFG NiTi with and without sol–gel coating in SBF are depicted by polarization curves in Fig. 4. Values of corrosion current density (i_{corr}), corrosion potential (E_{corr}) and pitting corrosion potential (E_{pit}) extracted from the curves are shown in Table 1.

Table 1
The calculated electrochemical parameter values.

Samples	E_{corr} (mV(SCE))	i_{corr} (μA/cm^2)	E_{pit} (mV(SCE))
CG NiTi	−294	4.40	534
UFG NiTi	−272	3.41	393
UFG NiTi with $SrO–SiO_2–TiO_2$ coating	−207	0.629	1800

The thin coatings of $SrO–SiO_2–TiO_2$ deposited by sol–gel methods on UFG NiTi acted very efficiently as corrosion protectors in SBF as demonstrated by the increase of E_{corr} from −207 mV(SCE) to 272 mV(SCE) and the decrease of i_{corr} from 3.41 μA/cm^2 to 0.629 μA/cm^2 after $SrO–SiO_2–TiO_2$ sol–gel was coated onto UFG NiTi. Especially, E_{pit} was significantly increased from 393 mV(SCE) to 1800 mV(SCE) with sol–gel coating, which means the sol–gel coating strongly enhanced the pitting corrosion resistance of UFG NiTi. It was reported that E_{pit} of NiTi was improved for about 200 mV by the sol–gel derived TiO_2 film [10]. Thus the increase of pitting corrosion resistance is more significantly for $SrO–SiO_2–TiO_2$ sol–gel coating in this study than sol–gel derived TiO_2 film. Meanwhile, the slight increase of E_{corr} and significant decrease of i_{corr} for the $SrO–SiO_2–TiO_2$ sol–gel coating on UFG NiTi in this study is similar to the corrosion behavior of sol–gel derived $TiO_2–SiO_2$ film on 316L stainless steel in H_2SO_4 solutions [11] The SEM surface morphologies of NiTi with and without sol–gel coating after electrochemical tests in Fig. 5 proved the above results. The corrosion pits were observed at the surface of CG NiTi and UFG NiTi after electrochemical tests (Fig. 5(a, b)) while UFG NiTi with sol–gel coating showed no pitting behavior and remained smooth under naked-eye examination. Only the breakage of sol–gel coating was observed after applied high voltage of 2000 mV during electrochemical tests (Fig. 5(c)). EDS results in Fig. 5(d) reveals that a little calcium phos-

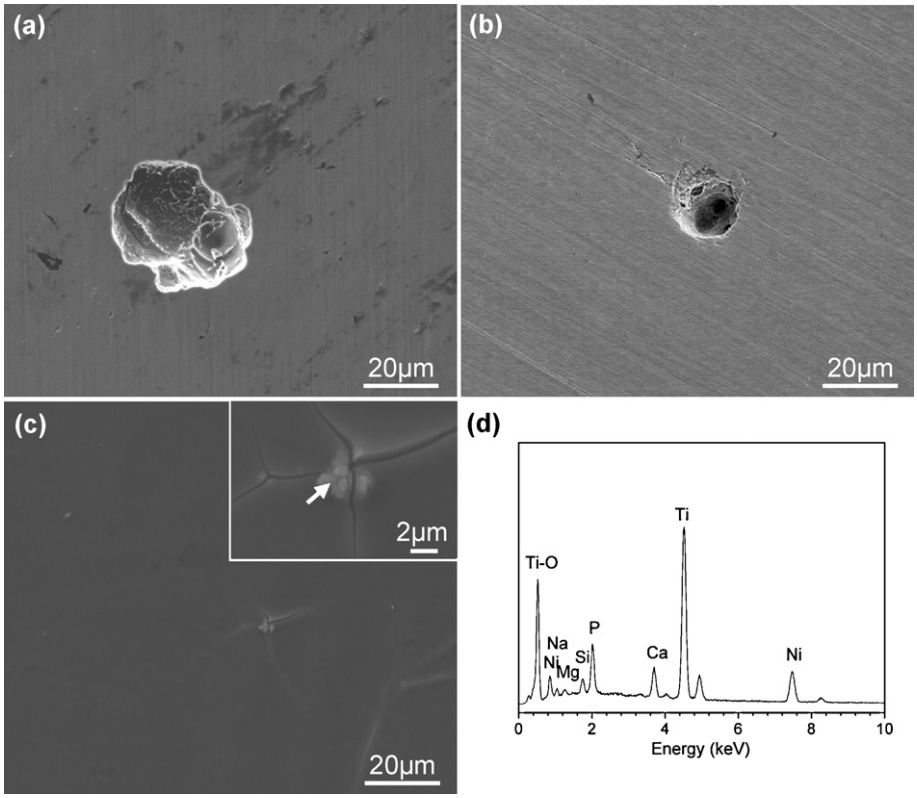

Fig. 5. SEM surface morphologies of (a) CG NiTi, (b) UFG NiTi without $SrO–SiO_2–TiO_2$ sol–gel coating and (c) UFG NiTi with $SrO–SiO_2–TiO_2$ sol–gel coating after electrochemical tests, with the high-magnification image as the inset on the upper-right corner, (d) EDS spectrum from the position marked by an arrow in the inset figure of (c).

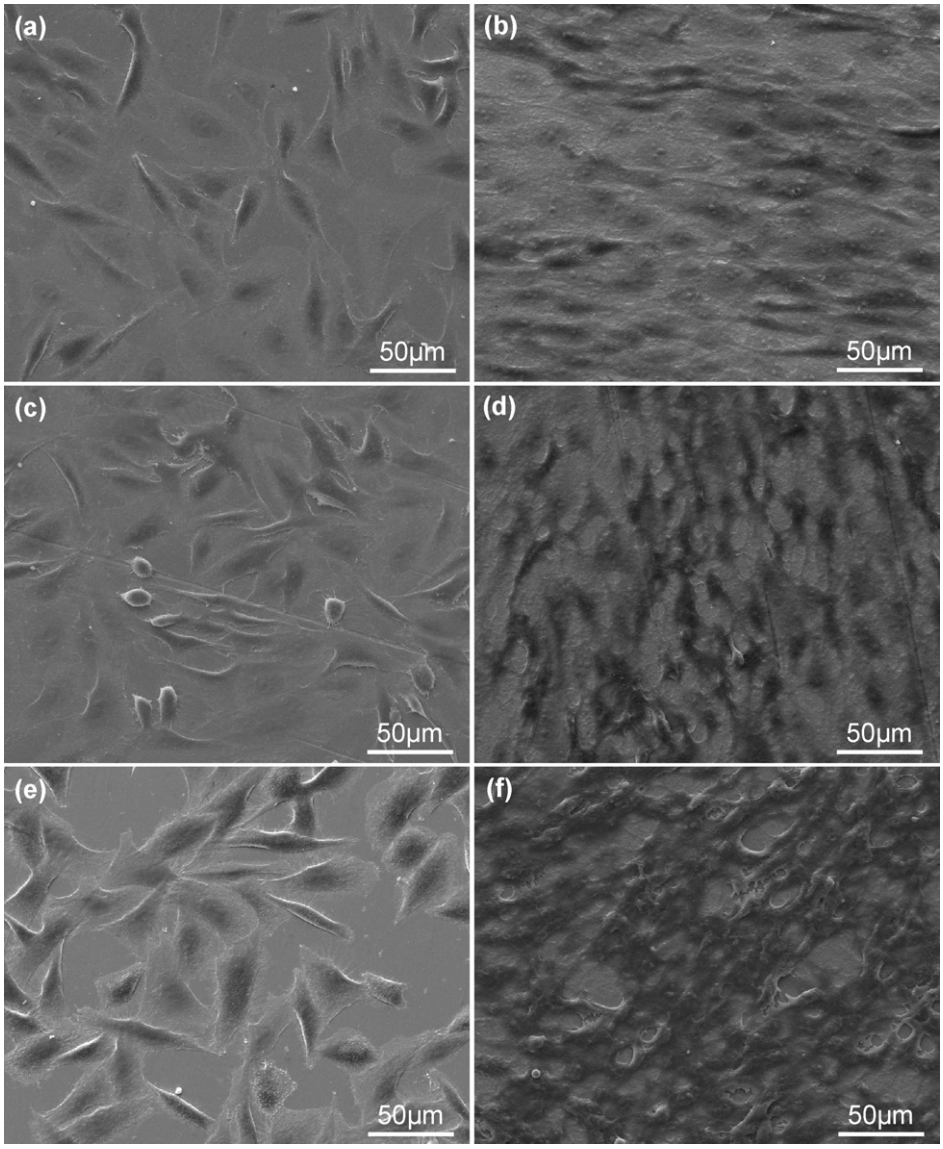

Fig. 6. The morphology of MG63 cells cultured on (a, b) CG-NiTi, (c, d) UFG-NiTi, (e, f) UFG-NiTi with SrO–SiO_2–TiO_2 sol–gel coating for 4 h (a, c, e) and 3 days (b, d, f).

phate with a trace of sodium and magnesium was adsorbed at the breakage site after electrochemical tests. The surfaces of UFG NiTi with coating were abundant of Si–OH and Ti–OH groups due to the hydrolysis of sol–gel coating. The bioactive hydroxyl groups could attract calcium and phosphate from the simulated body fluid and form bone-like calcium phosphate on the surface, thus promoting bone bonding [15,26]. This shows, from one aspect, that the SrO–SiO_2–TiO_2 sol–gel coating on UFG NiTi is bioactive.

3.3. Cell behavior

Fig. 6 shows the morphologies of MG 63 cells cultured on CG NiTi and UFG NiTi with and without sol–gel coating for different time. It can be shown that MG 63 cells attached well after 4 h culture, and proliferated well after 3 days culture on all the studied sample surfaces (Fig. 6(a, b)). Differently, the cells on UFG NiTi with sol–gel coating (Fig. 6(c)) were bigger and more spreading than those on UFG NiTi at 4 h culture. After 3 days culture, there were more cells on coated UFG NiTi (Fig. 6(d)) compared to uncoated UFG NiTi. Thus, SrO–SiO_2–TiO_2 coating enhanced the cell attachment, spreading and proliferation of UFG NiTi.

A variety of oxide coatings on titanium and other biomedical alloy substrates produced by the sol–gel process have been investigated in order to take advantage of their potential resistance to corrosion and excellent biocompatibility. Sol–gel-derived titania was reported to be compatible with bone cells and is able to facilitate osteogenesis of bone precursor cells [27]. However, it showed no advantages in initial cell adhesion and growth. Differently, Advincula et al. [19] found there were more osteoblastic cells adhered to the sol–gel derived titania coated Ti6Al4 V surface compared with that passivated with 30% HNO_3. And Ochsenbein et al. [14] compared the cell proliferation rates of four different sol–gel coatings, which is SiO_2–TiO_2, TiO_2, Nb_2O_5 and SiO_2, and found out that SiO_2–TiO_2 sol–gel coating is the highest. Their work also indicated that the chemical composition of the surface coating rather than the other physicochemical parameters was essential to the cell reactions. In this study, osteoblast-like cell attachment as well as cell proliferation was enhanced by SrO–SiO_2–TiO_2 coating. Areva et al. [28] revealed that TiO_2–SiO_2 (70:30) was the best for fibroblasts and TiO_2–SiO_2 (30:70) for osteoblasts. However, considering the remarkable differences of thermal expansion coefficient of SiO_2 with TiO_2 and titanium or titanium alloy substrate, the content of SiO_2 in sol–gel coating should be strictly controlled to avoid

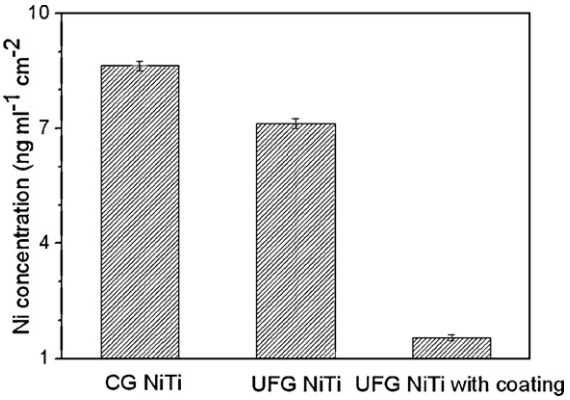

Fig. 7. The release of Ni ions of CG-NiTi and UFG-NiTi with and without $SrO–SiO_2–TiO_2$ sol–gel coating.

internal stress because of the mismatch of thermal expansion coefficient. In this study, the content of SiO_2 was limited to be slightly lower than 30%. Bending test has already shown that the adhesion between NiTi and sol–gel derived titania-silica coating with the molar ratio of 70:30 was sufficient [29]. The excellent osteoblast-like cell behavior in this study was achieved by introducing a small amount of SrO to $SiO_2–TiO_2$ sol system. Strontium is another ion that plays a key role in cell activation mechanisms by controlling many growth-associated processes and functional activities of cells. The beneficial effect of Sr on bone formation and healing osteoporotic has been extensively reported [16,30]. Hesaraki et al. [30] found that the proliferation and alkaline phosphatase activity of osteoblastic cells on $CaO–SrO–SiO_2–P_2O_5$ glass were higher than those bioactive glasses without SrO and glasses with high dose of Sr. Thus, the incorporation of a small amount of SrO to $SiO_2–TiO_2$ sol system enhanced the osteoblast-like cell behavior in this study. Meanwhile, the $SrO–SiO_2–TiO_2$ sol–gel coating on UFG NiTi significantly decreased the releasing rate of Ni ions (Fig. 7), which would further increase the cytocompatibility of UFG NiTi. In general, the positive effect of SrO on bone forming cells, together with blocking effect on Ni ion release enhanced the cellular behavior of UFG NiTi with $SrO–SiO_2–TiO_2$ sol–gel coating.

4. Conclusions

A novel, homogeneous and smooth $SrO–SiO_2–TiO_2$ sol–gel coating without cracks was fabricated on UFG NiTi surface. The sol–gel coating significantly increased the corrosion resistance and decreased the release of nickel ions of UFG NiTi. UFG NiTi with sol–gel coating exhibited enhanced osteoblast-like cell attachment, spreading and proliferation compared with that without coating and CG NiTi.

Acknowledgements

This work was supported by the NSFC-RFBR Cooperation Project (2010–2011, grant no. 31011120091), National Natural Science Foundation of China (no. 51041004), State Key Development Program for Basic Research of China (grant 2007CB936103), Beijing Municipal Natural Science Foundation (2082010), and theFundamental Research Funds for the Central Universities (grant PKUJC2009001).

References

[1] D. Mantovani, Shape memory alloys: properties and biomedical applications, JOM 52 (10) (2000) 36–44.
[2] V.G. Pushin, V.V. Stolyarov, R.Z. Valiev, T.C. Lowe, Y.T. Zhu, Nanostructured TiNi-based shape memory alloys processed by severe plastic deformation, Mater. Sci. Eng. A 410–411 (2005) 386–389.
[3] S. Faghihi, A.P. Zhilyaev, J.A. Szpunar, F. Azari, H. Vali, M. Tabrizian, Nanostructuring of a titanium material by high-pressure torsion improves pre-osteoblast attachment, Adv. Mater. 19 (8) (2007) 1069–1073.
[4] E. Prokofyev, D. Gunderov, S. Prokoshkin, R.Z. Valiev, Microstructure, mechanical and functional properties of NiTi alloys processed by ECAP technique, ESOMAT 06028 (2009).
[5] T.N. Kim, A. Balakrishnan, B.C. Lee, W.S. Kim, K. Smetana, J.K. Park, B.B. Panigrahi, In vitro biocompatibility of equal channel angular processed (ECAP) titanium, Biomed. Mater. 2 (3) (2007) S117–120.
[6] V.V. Stolyarov, Y.T. Zhu, I.V. Alexandrov, T.C. Lowe, R.Z. Valiev, Grain refinement and properties of pure Ti processed by warm ECAP and cold rolling, Mater. Sci. Eng. A 343 (1–2) (2003) 43–50.
[7] A.V. Sergueeva, C. Song, R.Z. Valiev, A.K. Mukherjee, Structure and properties of amorphous and nanocrystalline NiTi prepared by severe plastic deformation and annealing, Mater. Sci. Eng. A 339 (1–2) (2003) 159–165.
[8] F.L. Nie, Y.F. Zheng, Y. Cheng, S.C. Wei, R.Z. Valiev, In vitro corrosion and cytotoxicity on microcrystalline, nanocrystalline and amorphous NiTi alloy fabricated by high pressure torsion, Mater. Lett. 64 (8) (2010) 983–986.
[9] G. Rondelli, Corrosion resistance tests on NiTi shape memory alloy, Biomaterials 17 (20) (1996) 2003–2008.
[10] J.X. Liu, D.Z. Yang, F. Shi, Y.J. Cai., Sol-gel deposited TiO_2 film on NiTi surgical alloy for biocompatibility improvement, Thin Solid Films 429 (1–2) (2003) 225–230.
[11] M. Atik, P.D. Neto, M.A. Aegerter, L.A. Avaca, Sol-gel TiO_2-SiO_2 films as protective coatings against corrosion of 316L stainless-steel in H_2SO_4 solutions, J. Appl. Electrochem. 25 (2) (1995) 142–148.
[12] S.K. Tiwari, T. Mishra, M.K. Gunjan, A.S. Bhattacharyya, T.B. Singh, R. Singh, Development and characterization of sol-gel silica-alumina composite coatings on AISI 316L for implant applications, Surf. Coat. Technol. 201 (16–17) (2007) 7582–7588.
[13] S. Nagarajan, N. Rajendran, Surface characterisation and electrochemical behaviour of porous titanium dioxide coated 316L stainless steel for orthopaedic applications, Appl. Surf. Sci. 255 (7) (2009) 3927–3932.
[14] A. Ochsenbein, F. Chai, S. Winter, M. Traisnel, J. Breme, H.F. Hildebrand, Osteoblast responses to different oxide coatings produced by the sol-gel process on titanium substrates, Acta Biomater. 4 (5) (2008) 1506–1517.
[15] R. Viitala, M. Jokinen, T. Peltola, K. Gunnelius, J.B. Rosenholm, Surface properties of in vitro bioactive and non-bioactive sol-gel derived materials, Biomaterials 23 (15) (2002) 3073–3086.
[16] S. Hesaraki, M. Gholami, S. Vazehrad, S. Shahrabi, The effect of Sr concentration on bioactivity and biocompatibility of sol-gel derived glasses based on CaO-SrO-SiO_2-P_2O_5 quaternary system, Mater. Sci. Eng. C 30 (3) (2010) 383–390.
[17] F.T. Cheng, P. Shi, H.C. Man., Anatase coating on NiTi via a low-temperature sol-gel route for improving corrosion resistance, Scripta Mater. 51 (11) (2004) 1041–1045.
[18] M. Jokinen, M. Patsi, H. Rahiala, T. Peltola, M. Ritala, J.B. Rosenholm, Influence of sol and surface properties on in vitro bioactivity of sol-gel-derived TiO_2 and TiO_2-SiO_2 films deposited by dip-coating method, J. Biomed. Mater. Res. A 42 (2) (1998) 295–302.
[19] M.C. Advincula, F.G. Rahemtulla, R.C. Advincula, E.T. Ada, J.E. Lemons, S.L. Bellis, Osteoblast adhesion and matrix mineralization on sol-gel-derived titanium oxide, Biomaterials 27 (10) (2006) 2201–2212.
[20] T. Kokubo, H. Takadama, How useful is SBF in predicting in vivo bone bioactivity? Biomaterials 27 (15) (2006) 2907–2915.
[21] H.J. Jeon, S.C. Yi, S.G. Oh., Preparation and antibacterial effects of Ag-SiO_2 thin films by sol-gel method, Biomaterials 24 (27) (2003) 4921–4928.
[22] M.F. Morks, Plasma spraying of zirconia-titania-silica bio-ceramic composite coating for implant application, Mater. Lett. 64 (18) (2010) 1968–1971.
[23] C. Trépanier, M. Tabrizian, L.H. Yahia, L. Bilodeau, D.L. Piron, Effect of modification of oxide layer on NiTi stent corrosion resistance, J. Biomed. Mater. Res. B 43 (4) (1998) 433–440.
[24] S.A. Shabalovskaya, G.C. Rondelli, A.L. Undisz, J.W. Anderegg, T.D. Burleigh, M.E. Rettenmayr, The electrochemical characteristics of native Nitinol surfaces, Biomaterials 30 (22) (2009) 3662–3671.
[25] N.K. Sarkar, W. Redmond, B. Schwaninger, A.J. Goldberg, The chloride corrosion behaviour of four orthodontic wires, J. Oral Rehabil. 10 (2) (1983) 121–128.
[26] D. Arcos, M. Vallet-Regi., Sol-gel silica-based biomaterials and bone tissue regeneration, Acta Biomater. 6 (8) (2010) 2874–2888.
[27] S.C. Dieudonné, J. van den Dolder, J.E. de Ruijter, H. Paldan, T. Peltola, M.A. van't Hof, R.P. Happonen, J.A. Jansen, Osteoblast differentiation of bone marrow stromal cells cultured on silica gel and sol-gel-derived titania, Biomaterials 23 (14) (2002) 3041–3051.
[28] S. Areva, V. Aaritalo, S. Tuusa, M. Jokinen, M. Linden, T. Peltola, Sol-Gel-derived TiO_2-SiO_2 implant coatings for direct tissue attachment Part II: Evaluation of cell response, J. Mater. Sci. Mater. Med. 18 (8) (2007) 1633–1642.
[29] V. Mulhonen, S. Kujala, A. Vuotikka, V. Ääritalo, T. Peltola, S. Areva, T. Närhi, J. Tuukkanen, Biocompatibility of sol-gel-derived titania-silica coated intramedullary NiTi nails, Acta Biomater. 5 (2) (2009) 785–793.
[30] S. Pors, Nielsen, The biological role of strontium, Bone 35 (3) (2004) 583–588.